CONF-920382--1

ANL/CP--72368

DE92 019037

THREE-DIMENSIONAL HYDRODYNAMIC AND EROSION MODELING OF FLUIDIZED BEDS USING KINETIC THEORY

by

Jianmin Ding,+ Robert W. Lyczkowski
ARGONNE NATIONAL LABORATORY
Energy Systems Division
+Materials and Components Technology Division
9700 South Cass Avenue
Argonne, IL 60439 USA

and

Steve W. Burge
BABCOCK & WILCOX
Alliance Research Center
1562 Beeson Street
Alliance, Ohio 44601-2196

Final Manuscript for
International Conference on Transport Phenomena in Processing
March 22-26, 1992
Waikiki, Hawaii

May, 1992

ABSTRACT

Three-dimensional hydrodynamic models for gas-solids flow are developed and used to compute bubble and solids motion in rectangular fluidized beds. Our computed results demonstrate the significance and necessity for three-dimensional models of hydrodynamics and erosion in fluidized-bed combustors. A kinetic theory model for erosion using Finnie's single-particle ductile erosion model was used to compute erosion in a rectangular fluidized bed containing a single tube. Comparison of two-dimensional and three-dimensional computed hydrodynamics, erosion rates, and patterns clearly show the superiority of three-dimensional modeling.

Introduction

Solids motion (and the associated bed dynamics involving bubble evolution and pressure fluctuations) is the key to understanding the erosion processes in fluidized-bed combustors (FBC's). Fluidized-bed combustors used in industry have continued to show promise for burning high sulfur coal, but erosion of in-bed tubes and other components is still hampering the commercialization of the FBC technology. Despite its importance, the exact mechanisms of erosion and hydrodynamics in fluidized beds are poorly understood. One reason may be due to the lack of three-dimensional models for fluidized-bed hydrodynamics and erosion models.

A three-dimensional model with a constant microscopic solids viscosity was used by Gidaspow and Ding (1990) to simulate gas-solids flow in a thin "two-dimensional" fluidized bed with a circular jet. To date, no published three-dimensional two-phase flow models have been used to simulate fluidized beds, to our knowledge. One reason is the extensive computing cost.

In this paper we present our three-dimensional models for fluidized beds and demonstrate the significance and the necessity of three-dimensional models of hydrodynamics and erosion. The computer codes used are FLUFIX (Lyczkowski and Bouillard, 1989), FORCE2 (Burge, 1991), and IFAP. The empirical models

Jianmin Ding and Robert W. Lyczkowski* — Argonne National Laboratory, Materials and Components Technology Division; Energy Systems Division*, 9700 South Cass Avenue, Argonne, IL 60439-4815

Steve W. Burge — Babcock & Wilcox, Alliance Research Center, 1562 Beeson Street, Alliance, Ohio 44601-2196

for solids viscosity and solids stress (Gidaspow, 1986; Lyczkowski and Bouillard, 1989; Bouillard et al., 1989) were used in FLUFIX and FORCE2. The kinetic theory granular two-phase flow model developed by Ding and Gidaspow (1990) was extended to three-dimensional in IFAP. A kinetic theory model for erosion using Finnie's (1960) single-particle ductile erosion model is used to compute erosion around tube surfaces in a rectangular fluidized bed. The computations show the significance of three-dimensional effects on bed dynamics and tube wear.

Governing Equations

Equations for Gas-Solids Flow

The gas phase flow can be assumed to be Newtonian. The transport equations for the solids phase were derived starting from the Boltzman equation for the velocity distribution of particles. The obtained continuity equations and momentum equations are listed in Table 1, Eqs. (T1) and (T2), respectively. The fluctuating solids phase kinetic energy equation is given in Eq. (T7) in Table 1.

To close the solids phase transport equations, we need constitutive relations for solids stresses and solids strain rates. The empirical solids viscosity and stress model were listed in Eqs. (T5a) to (T5d). In the kinetic theory, we assumed the single particle velocity distribution function to be Maxwellian (Ding and Gidaspow, 1990; Jenkins and Savage, 1983),

$$f(\mathbf{r}.\mathbf{c},t) = \frac{n}{(2\pi T)^{\frac{3}{2}}} exp[-\frac{(\mathbf{c}-\mathbf{v_s})^2}{2T}] \tag{1}$$

where $\mathbf{c}$ is the instantaneous particle velocity, n is the particle number density, T is the granular temperature, and $\mathbf{v_s}$ is the mean solids velocity, and used the Enskog assumption for the pair-distribution function (Chapman and Cowling, 1976). The constitutive equations obtained are listed in in Eqs. (6a) to (T6d) in Table 1. In Eq.(T7), the correlation between the gas phase fluctuation velocity and the solids phase fluctuation velocity has been neglected, as discussed by Ding and Gidaspow (1990). The radial distribution function, g_0, listed in Eq. (T6d) was recommended by Lun and Savage (1986) to match the data of Alder and Wainwright (1960) more closely.

Eq. (1) has implied three-dimensional fluctuation flow of particles. Two-dimensional fluctuation of particles cannot really exist. From this point of view, the three-dimensional model must be used as shown in this paper.

Boundary Conditions

To solve the three dimensional equations of gas-solids flow given above, we need appropriate initial conditions and boundary conditions for the two-phase velocities, the gas phase pressure, the porosity, and the granular temperature. The initial conditions depend upon the problem investigated. The inlet conditions are usually given. For example, the porosity is set to 1 where particle-free gas enters the system. The boundary conditions at planes of symmetry demand zero normal gradient of all variables.

At an impenetrable solid wall, the gas phase velocities in the three normal and tangential directions are set to zero. The no-slip condition cannot always be applied to the solids phase. Since the particle diameter is usually larger than the length scale of surface roughness of the rigid wall, the particles may partially slip

TABLE 1. GOVERNING EQUATIONS FOR GAS-SOLIDS FLOW

1. CONTINUITY EQUATION FOR PHASE $k(= g, s)$

$$\frac{\partial}{\partial t}(\epsilon_k \rho_k) + \nabla \cdot (\epsilon_k \rho_k \mathbf{v_k}) = 0 \qquad (T1)$$

$$\sum_k \epsilon_k = 1 \qquad (T1a)$$

2. MOMENTUM EQUATION FOR PHASE $k(= g, s; l = g, s; l \neq k)$

$$\frac{\partial}{\partial t}(\epsilon_k \rho_k \mathbf{v_k}) + \nabla \cdot (\epsilon_k \rho_k \mathbf{v_k} \mathbf{v_k}) = -\epsilon_k \nabla p_g + \epsilon_k \rho_k \mathbf{g} + \nabla \cdot \bar{\bar{\tau}}_k + \beta(\mathbf{v_l} - \mathbf{v_k}) \quad (T2)$$

3. GAS PHASE STRESS

$$\bar{\bar{\tau}}_g = 2\epsilon_g \mu_g \bar{\bar{\mathbf{S}}}_g \qquad (T3)$$

where

$$\bar{\bar{\mathbf{S}}}_g = \frac{1}{2}[\nabla \mathbf{v_g} + (\nabla \mathbf{v_g})^T] - \frac{1}{3} \nabla \cdot \mathbf{v_g} \qquad (T3a)$$

4. SOLIDS PHASE STRESS

$$\bar{\bar{\tau}}_s = [-p_s + \epsilon_s \xi_s \nabla \cdot \mathbf{v_s}]\bar{\bar{\mathbf{I}}} + 2\epsilon_s \mu_s \bar{\bar{\mathbf{S}}}_s \qquad (T4)$$

Deformation Rate

$$\bar{\bar{\mathbf{S}}}_s = \frac{1}{2}[\nabla \mathbf{v_s} + (\nabla \mathbf{v_s})^T] - \frac{1}{3} \nabla \cdot \mathbf{v_s} \bar{\bar{\mathbf{I}}} \qquad (T4a)$$

5. EMPIRICAL SOLIDS VISCOSITY AND STRESS MODEL

$$\xi_s = 0 \qquad (T5a)$$

$$\nabla p_s = G(\epsilon_s) \nabla \epsilon_s \qquad (T5b)$$

$$G(\epsilon_s) = exp[-600(\epsilon - 0.376)] \qquad (T5c)$$

$$\mu_s = 5 Pa \cdot s \qquad (for\ \ example) \qquad (T5d)$$

6. KINETIC THEORY MODEL

Solids Phase Pressure

$$p_s = \epsilon_s \rho_p [1 + 2(1 + e)\epsilon_s g_0] T \qquad (T6a)$$

Solids Phase Bulk Viscosity

$$\xi_s = \frac{4}{3} \epsilon_s \rho_p d_p g_0 (1 + e)(\frac{T}{\pi})^{\frac{1}{2}} \qquad (T6b)$$

Solids Phase Shear Viscosity

$$\mu_s = \frac{4}{5} \epsilon_s \rho_p d_p g_0 (1 + e)(\frac{T}{\pi})^{\frac{1}{2}} \qquad (T6c)$$

Radial Distribution Function

$$g_0 = (1 - \frac{\epsilon_s}{\epsilon_{smax}})^{-2.5\epsilon_{smax}} \qquad (T6d)$$

TABLE I. (*continued*)
Fluctuating Energy $\frac{3}{2}T$ $(= \frac{1}{2} < C^2 >)$ Equation

$$\frac{3}{2}[\frac{\partial}{\partial t}(\epsilon_s \rho_p T) + \nabla \cdot (\epsilon_s \rho_p \mathbf{v_s} T)] = \bar{\bar{\tau}}_\mathbf{s} : \nabla \mathbf{v_s} - \nabla \cdot \mathbf{q} - \gamma - 3\beta T \qquad (T7)$$

Collisional Energy Dissipation γ

$$\gamma = 3(1-e^2)\epsilon_s^2 \rho_p g_0 T[\frac{4}{d_p}(\frac{T}{\pi})^{\frac{1}{2}} - \nabla \cdot \mathbf{v_s}] \qquad (T7a)$$

Flux of Fluctuating Energy $\mathbf{q}$

$$\mathbf{q} = -\kappa \nabla T \qquad (T7b)$$

Conductivity of the Fluctuating Energy

$$\kappa = 2\rho_p \epsilon_s^2 d_p (1+e) g_0 (\frac{T}{\pi})^{\frac{1}{2}} \qquad (T7c)$$

7. GAS-SOLIDS DRAG COEFFICIENTS

For $\epsilon \leq 0.8$,

$$\beta = 150\frac{\epsilon_s^2 \mu_g}{\epsilon(d_p \phi_s)^2} + 1.75\frac{\rho_g \epsilon_s |\mathbf{v}_g - \mathbf{v}_s|}{d_p \phi_s} \qquad (T8)$$

For $\epsilon > 0.8$,

$$\beta = \frac{3}{4} C_d \frac{\epsilon \epsilon_s \rho_g |\mathbf{v}_g - \mathbf{v}_s|}{d_p \phi_s} \epsilon^{-2.65} \qquad (T9)$$

where,

$$C_d = \frac{24}{Re_p}[1 + 0.15 Re_p^{0.687}], \quad For \quad Re_p \leq 1000 \qquad (T10)$$

$$C_d = 0.44, \quad for \quad Re_p > 1000, \qquad (T11)$$

$$Re_p = \frac{\epsilon \rho_g |\mathbf{v}_g - \mathbf{v}_s| d_p \phi_s}{\mu_g} \qquad (T12)$$

at the wall. This mean slip velocity can be assumed to be given by (Ding and Gidaspow, 1990),(Ding, 1990)

$$v_{s2}|_w = -\lambda_p \frac{\partial v_{s2}}{\partial x_1}|_w \tag{2}$$

where the x_1 direction is normal to the wall and the x_2 direction is tangential to the wall. The slip parameter, λ_p, is taken to be the mean distance between particles. In FORCE2 and FLUFIX, the mean free path is determined by

$$\lambda_p = \frac{d_p \phi_s}{\sqrt{2}\epsilon_s} \tag{2a}$$

where d_p is the particle diameter, ϕ_s is the sphericity of a particle, and ϵ_s is the solids volume fraction. In IFAP, λ_p is obtained from the expression

$$\lambda_p = < C^2 >^{\frac{1}{2}} \tau = (3T)^{\frac{1}{2}} \frac{n}{N_{pc}} \tag{3}$$

to give

$$\lambda_p = \sqrt{\frac{3\pi}{24}} \frac{d_p}{\epsilon_s g_0} \tag{4}$$

where τ is the time interval between particle collisions, C is the particle fluctuation velocity, T is the granular temperature, n is the particle number density, and N_{pc} is the number of particle collisions per unit time and unit volume,

$$N_{pc} = \int_{\mathbf{c_{12}}\cdot\mathbf{k}>0} (\mathbf{c_{12}} \cdot \mathbf{k}) d_p^2 f^{(2)}(\mathbf{r}, \mathbf{c_1}; \mathbf{r} + d_p\mathbf{k}, \mathbf{c_2}; t) d\mathbf{k} d\mathbf{c_1} d\mathbf{c_2} = 4\sqrt{\pi} d_p^2 g_0 n^2 T^{\frac{1}{2}} \tag{5}$$

The subscripts 1 and 2 denote particles 1 and 2. $\mathbf{c_{12}}$ is the relative velocity of particle 1 and particle 2, $f^{(2)}$ is the pair-distribution function, $\mathbf{k}$ is the unit vector from the center of particle 1 to the center of particle 2 at a collision, and d_p is the particle diameter. Note that for small particles or for a high solids concentration near the wall, the boundary condition of solids velocity is close to the no-slip conditions.

In IFAP, we simply assume zero gradient of granular temperature at the wall.

Kinetic Theory for Erosion

Finnie's single-particle erosion model (1960) accounts for ductile erosion caused by a single particle. The volume removed by erosion, W, in Finnie's model is given as a function of the particle's instantaneous speed near the wall, c_w, angle of attack, α, and mass, m, and is given by

$$W = B_F m c_w^2 f(\alpha) \tag{6}$$

where

$$B_F = \frac{C_F}{P_H \zeta K} \tag{7}$$

and

$$f(\alpha) = \begin{cases} \sin 2\alpha - \frac{6}{K}\sin^2\alpha, & \alpha \le \tan^{-1}\frac{K}{6}; \\ \frac{K}{6}\cos^2\alpha, & \alpha > \tan^{-1}\frac{K}{6} \end{cases} \tag{8}$$

P_H is the Vickers hardness of the target surface, C_F is the model constant, ζ is the ratio of the depth of contact to the depth of cut, and K is the ratio of the vertical to the horizontal force. $\mathbf{c}_w$ is the particle impact velocity at the wall. According to Finnie (1960), B_F is

$$B_F = \frac{1}{8P_H} \tag{9}$$

and

$$f(\alpha) = \begin{cases} \sin 2\alpha - 3\sin^2\alpha, & \alpha \le 18.43^o; \\ \frac{1}{3}\cos^2\alpha, & \alpha > 18.43^o \end{cases} \tag{10}$$

The erosion rate of a solid wall surface caused by multi-particle impacts, $\dot{E}$, can be obtained by integrating of the probability of finding particles within the range $\mathbf{c}$ to $\mathbf{c} + \mathbf{dc}$ per unit volume near the surface times erosion caused by one particle impact over all impact velocities in the range of $(-\infty, \infty)$ to obtained

$$\dot{E} = \int_{\mathbf{c}_w \cdot \mathbf{n} > 0} (\mathbf{c}_w \cdot \mathbf{n}) B_F m \mathbf{c}_w{}^2 f(\alpha) f_w(\mathbf{r}, \mathbf{c}, t) d\mathbf{c}_w \tag{11}$$

where the single-particle velocity distribution function f_w near the wall is assumed to be Maxwellian. The particle's fluctuating velocity near the wall is given as the difference between the instantaneous and mean velocities as

$$\mathbf{C}_w = \mathbf{c}_w - \mathbf{v}_w \tag{12}$$

At an impenetrable wall, the mean normal velocity of solids is zero. However by eq.(12) the mean tangential velocity may not be zero if there is partial slip of particles at the wall. The integration yields (Ding and Lyczkowski, 1991)

$$\dot{E} = 2\epsilon_s \rho_p B_F \left[\frac{(2T)^{\frac{3}{2}}}{\sqrt{\pi}} F_1(\theta_c) + \frac{v_w^2}{2}\sqrt{\frac{2T}{\pi}} F_1(\theta_c) + \frac{3}{2} v_w T F_2(\theta_c)\right] \tag{13}$$

where

$$F_1(\theta_c) = \frac{\pi}{8} - \frac{\theta_c}{4} + \frac{1}{12}\sin^4\theta_c + \frac{1}{16}\sin 4\theta - \frac{3}{4}\cos^4\theta_c = 0.10 \tag{13a}$$

and

$$F_2(\theta_c) = -\frac{2}{5} + \frac{1}{15}\sin^5\theta_c - \frac{2}{5}\cos\theta_c \sin^4\theta_c + \frac{2}{15}(cos\theta_c \sin^2\theta_c + 2\cos\theta_c) + \frac{3}{5}\cos^2\theta_c \sin^3\theta_c + \frac{2}{5}\sin^3\theta_c = 0.06 \tag{13b}$$

Similar approach has been used by Rogers (1989) to derive an erosion model by combining Finnie's model with a kinetic theory granular flow model. In his derivation, Rogers used Taylor series expansions for the terms involving the exponential in the integration. However, no computation results were presented.

FORCE2 Computer Code Predictions

The FORCE2 computer code is an extension of an existing B & W (Burge, 1991) multidimensional, two-phase flow program. The conventional two-fluid hydrodynamic models (Gidaspow, 1986; Lyczkowski et al., 1986), which were used in FLUFIX two-dimensional computer code for fluid-solids flow, were implemented in FORCE2. The models have been extended in FORCE2 to include 1) three-dimensional cartesian geometries, and 2) volume porosities and surface permeabilities to account for volume and surface obstruction in the flow field.

The FORCE2 code was used to compute bed dynamics in a thin 40×3.81 cm fluidized bed with a jet velocity of 5.78 m/s. A rectangular obstacle was placed in the bed as shown in Figure 1. The bed materials are glass beads with a diameter of 500 μm and a density of 2.5 g/cm^3. Three slices were used in the depth direction of the bed. Figure 1 shows the FORCE2 three-dimensional predictions of time-averaged porosity contour and solids velocity in the bed. No significant difference in the depth direction were found in this "two-dimensional bed". Figure 2 shows the comparisons of FORCE2 predicted sliced-averaged porosities and solids velocities with Argonne National Laboratory's FLUFIX computed results. Both codes give similar solids flow patterns. However, differences in porosity distribution are noted.

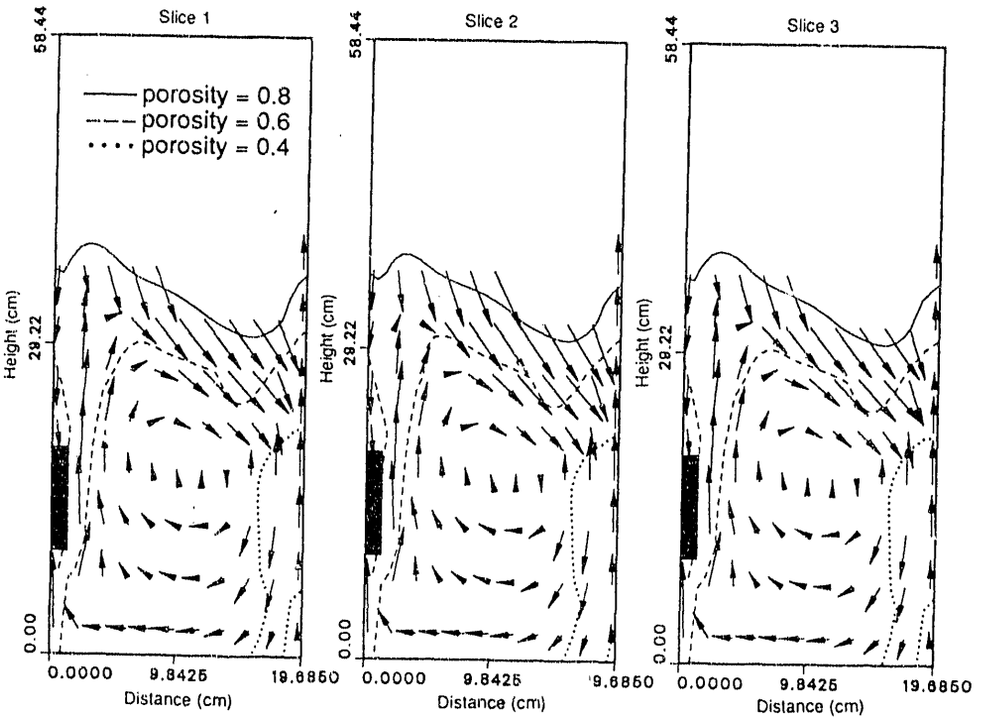

Figure 1. FORCE2 prediction: three-dimensional time-averaged (over 1 s) porosity contour and solids velocity in the thin 40×3.81 cm fluidized bed.

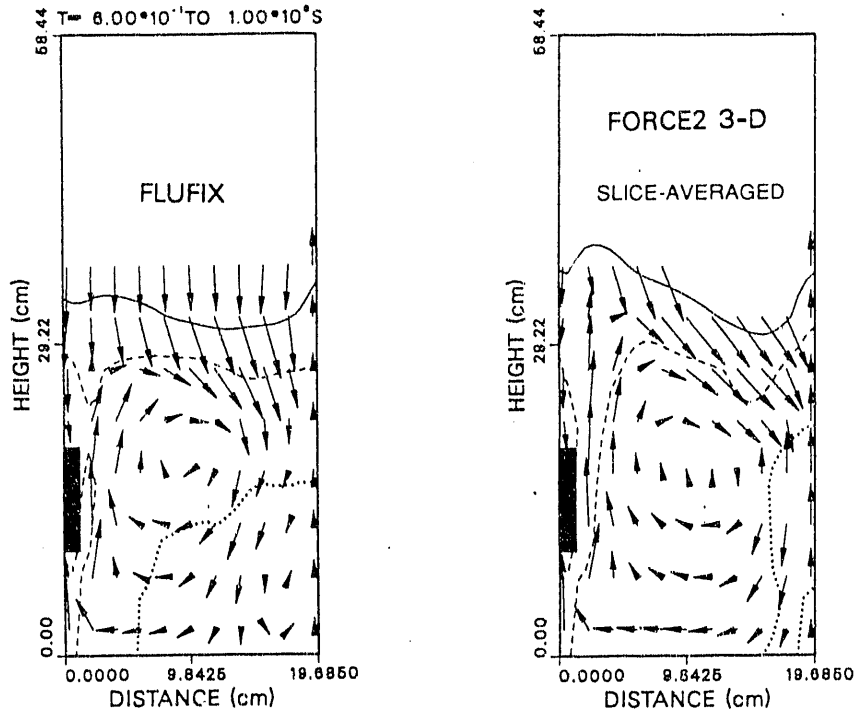

Figure 2. Comparison of FLUFIX (2-D) and FORCE2 (3-D) predictions: time-averaged porosity contour and solids velocity in the thin 40×3.81 cm fluidized bed.

IFAP Predictions

The two-dimensional IFAP (Isothermal Flow Analysis Program), which generalizes the FLUFIX code (Lyczkowski et al., 1986) used at Argonne National Laboratory (ANL) by adding a kinetic theory granular flow model and other features (Ding, 1990),(Ding and Gidaspow, 1990), was extended to a three-dimensional code for fluid-solids flow. The IFAP code has been demonstrated to be adaptable to a variety of problems including industrial-scale circulating fluidized bed (Ding,1990; Gidaspow et al., 1990) and liquid-solids flow (Gidaspow et al., 1991). The gas-solids bubbling fluidized bed erosion data of Zhu et al. (1990) were simulated in two- and three-dimensions.

Figure 3 shows a sketch of the fluidized bed used in the simulations assuming a quarter symmetry. A tube of $3.2 \times 3.2 \times 20.3 cm^3$ was used in the computation instead of a round tube with a diameter of 3.2 cm used in the experiment to reduce the number of finite difference cells. The bed materials are silica sand with a mean particle diameter of 1 mm, shape factor, ϕ_s, of 0.89 and a density of 2.58 g/cm^3. The initial bed height was 32 cm. The minimum fluidization velocity, U_{mf}, is 56 cm/s. The fluidizing velocity was 187 cm/s. Nonuniform grids were used in the computations, 10 in x direction, 43 in z direction and 4 in y direction for total of 1720. The influence of the grid size on the computed results of a two-dimensional

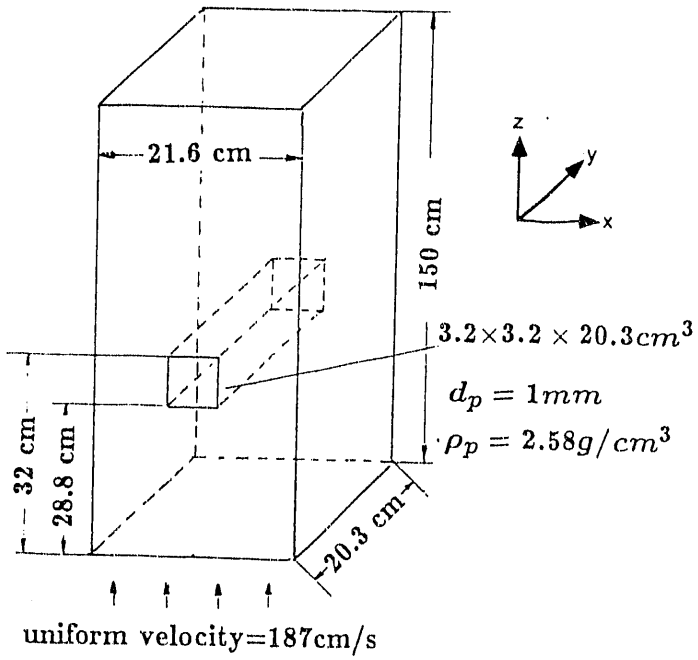

Figure 3. Three-dimensional fluidized bed with conditions used in computation.

1720. The influence of the grid size on the computed results of a two-dimensional fluidized bed has been checked by Ding and Gidaspow (1990). The hydrodynamic computations contained in this paper were performed on ANL's CRAY-XMP/14 and the erosion computations were post-processed on ANL's VAX 8700.About 15 hours of cpu time were required for three-dimensional hydrodynamic computation to reach 2 seconds of real transient time.

Figure 4 shows the computed time-averaged porosity contours and solids velocities. The time-averaging period was taken from 1.6 seconds to 2.0 seconds. The three-dimensional bubbles can be visualized by the four slices in the y direction, as shown in the figures. Bubble shapes, sizes, rising velocities, and bursting times are quite different due to the wall resistance to the solids and gas motion. The significance of the three-dimensional hydrodynamic simulation can be seen by comparing the three-dimensional results with the two-dimensional results using the same grid sizes. The two-dimensional time-averaged porosities and solids velocities were compared to three-dimensional time- and slice-averaged porosities and solids velocities, as shown in Figure 5. Completely different porosity contours and slightly different solids flow pattern were found.

Computed Erosion Rates

The erosion model was used to compute erosion rates of tube surfaces in the three-dimensional bed. Figure 6 shows the comparisons of computed time- and surface-averaged erosion rates as a function of tube material hardness with experimental data of Zhu et al. (1990). Both two- and three-dimensional predicted erosion rates reasonably match the experimental data. However, the three-

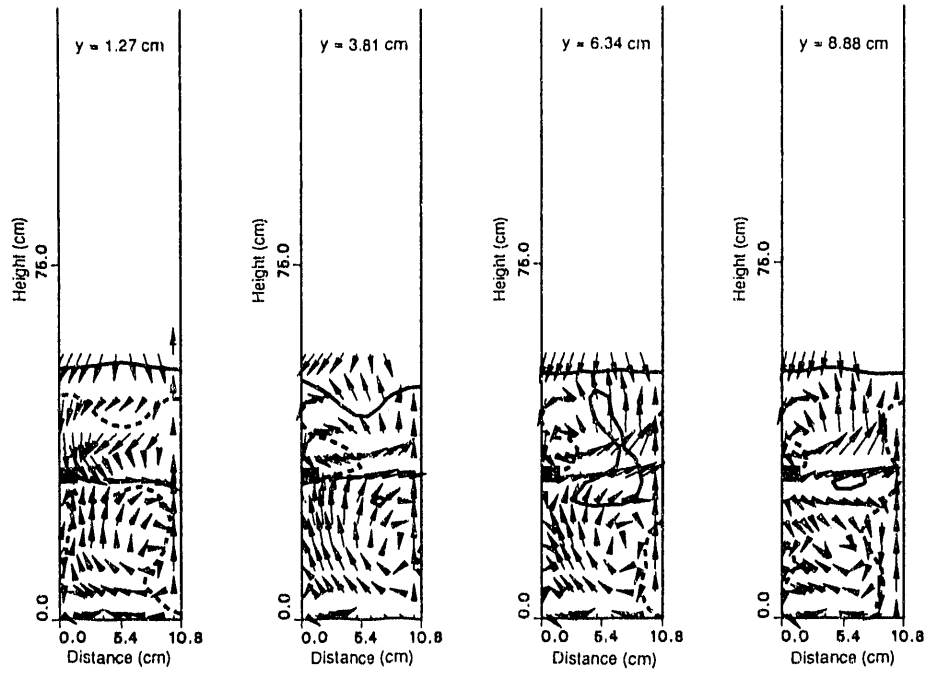

Figure 4. IFAP (3-D) predictions: time-averaged porosity contours and solids velocities in the three-dimensional bed.

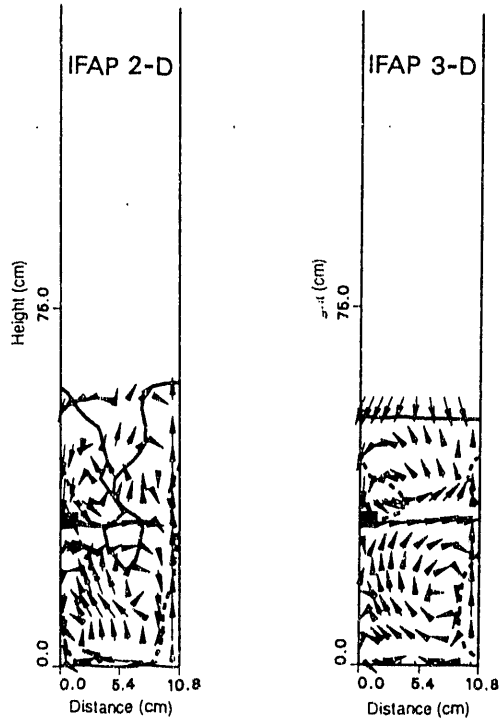

Figure 5. IFAP predictions: comparisons of time-averaged two- and three-dimensional silce-averaged porosity contours and solids velocities.

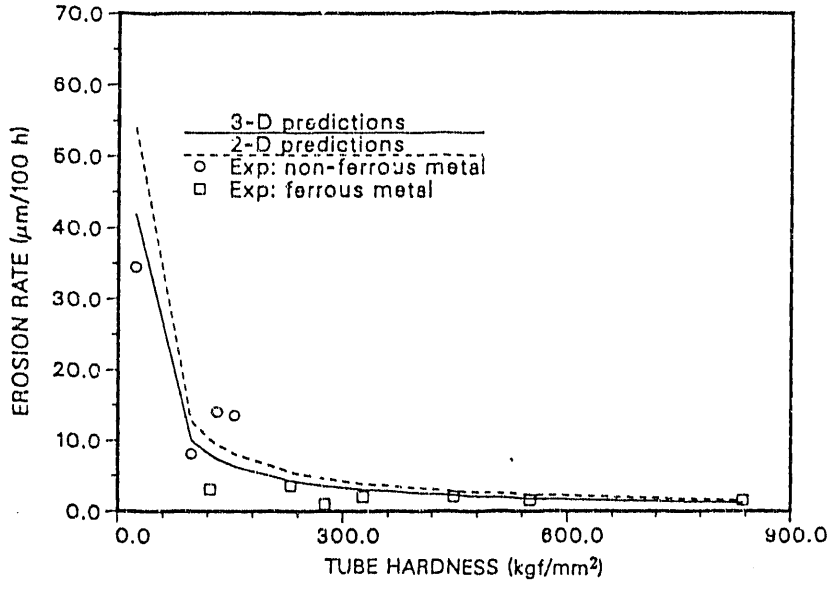

Figure 6. Comparisons of computed time-averaged erosion rates as a function of tube hardness with experimental data of Zhu et al.(1990). Fluidizing Velocity=187 cm/s, Particle Diameter=1 mm, Shape factor=0.86.

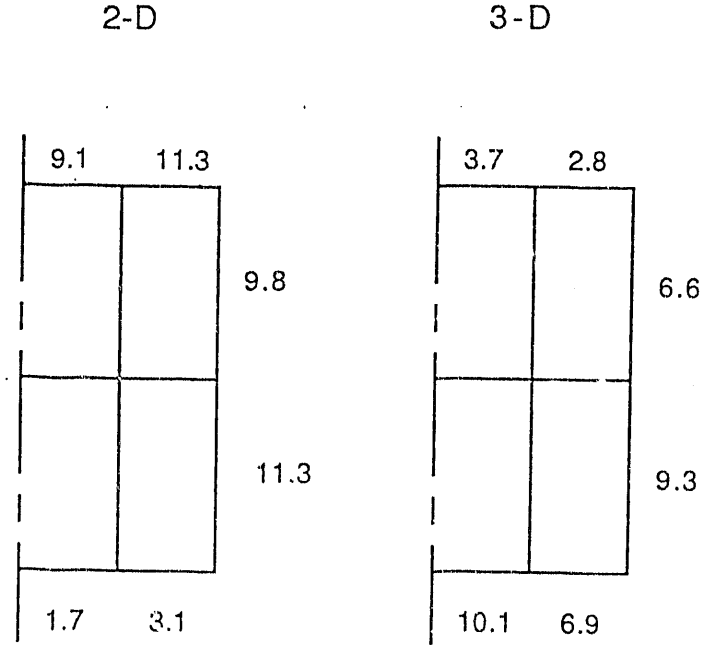

Figure 7. Comparisons of time-averaged two- and three-dimensional slice-averaged erosion rates ($\mu m/100$ hours) at each brass tube surface.

dimensional predictions generally agree better with the experiments. The computed two-dimensional and three-dimensional slice-averaged erosion rates at each tube surface are compared in Figure 7. Zhu et al. (1990) and other investigators (Stringer and Wright, 1986; Wood and Woodford, 1983) found that the highest erosion occurred near the tube's bottom and there was very low erosion at the tube's top. The erosion pattern of the three-dimensional predictions qualitatively agrees with these experiments. The two-dimensional results, however, do not give this erosion pattern. Therefore, the two-dimensional model is not as good as the three-dimensional model to compute local erosion rates.

Conclusions

Three-dimensional hydrodynamic models have been developed for gas-solids flow in fluidized beds. These models predict three-dimensional bubbles in a fluidized bed. Comparisons of predicted erosion patterns of three- and two-dimensional models with experiments again shows the importance of three-dimensional models. Based on our computer codes' three-dimensional features needed in modeling large fluidized-bed combustors, prediction and validation for many industrial application are possible now.

Acknowledgements

This study was supported under the Cooperative R&D Venture "Erosion of FBCS Heat Transfer Tubes", Contract W-31-109-ENG-38. Members are the U.S. Department of Energy, Morgantown Energy Technology Center (METC). Electric Power Research Institute (EPRI), State of Illinois Center for Research on Sulfur in Coal, Forster Wheeler Development Corp., ASEA Babcock PFBC, ABB Combustion Engineering Inc., Tennessee Valley Authority, and Argonne National Laboratory.

REFERENCES

Alder,B.J. and Wainwright,T.E. (1960). Studies in Molecular Dynamics. II: Behaviour of a Small Number of Elastic Spheres. *J. Chem. Phys.*, **33**, 1439-1451.

Bouillard,J.X., Lyczkowski,R.W., and Gidaspow,D. (1989). Porosity Distributions in a Fluidized Bed with an Immersed Obstacle. *AIChE J.* **35**, no.6, 908-922

Burge,S. FORCE2-A Multidimensional Flow Program for Gas Solids Flow, Theory and Users Guide. Babcock and Wilcox, Alliance,Oh.

Chapman,S. and Cowling,T.G.(1970). The Mathematical Theory of Non-Uniform Gases. 3rd edn. Cambridge Univ. Press.

Ding,J.(1990). *A Fluidization Model Using Kinetic Theory of Granular Flow.* Ph.D. Thesis, Illinois Institute of Technology, Chicago.

Ding,J. and Gidaspow, D. (1990). A Bubbling Fluidization Model Using Kinetic Theory of Granular Flow. *AIChE J.*, **36** no.4, 523-538.

Finnie,I. (1960). Erosion of Surfaces by Solid Particles. *Wear*, **3**, 87-103.

Gidaspow,D.(1986). Hydrodynamics of Fluidization and Heat Transfer: Supercomputer Modeling. *Appl. Mech. Rev.*, bf 39, no.1, 1-23.

Gidaspow,D., Jayaswal,U.K., and Ding,J.(1991). Navier-Stokes Equation Model for Liquid-Solid Flows Using Kinetic Theory. *Liquid-Solid Flows - 1991*, FED-Vol. 118, (ed. M.C.Roco and T.Masuyama), 165-172.

Gidaspow,D. and Ding,J.(1990). Predictive Models for Circulating Fluidized Bed Combustors, Three-Dimensional Code. DOE Report, DOE/PC/89769-T1, March, 1990.

Gidaspow,D., Ding,J., and Jayaswal,U.K. (1990). Multiphase Navier-Stokes Equation Solver. Numerical Methods for Multiphase Flows FED-Vol.91 (ed. I.Celik, D.Hughes, C.T. Crowe, and D.Lankford), 47-56.

Jenkins,J.T. and Savage,S.B.(1983). A Theory for the Rapid Flow of Identical,Smooth,Nearly Elastic,Spherical Particles. *J.Fluid Mech.*, **130**, 187-202.

Lun,C.K.K. and Savage,S.B. (1986). The Effects of an Impact Velocity Dependent Coefficient of Restitution on Stresses Developed by Sheared Granular Materials. *Acta Mechanica*, **63**, 15-44.

Lyczkowski,R.W. and Bouillard,J.X. Interim Users Manual for FLUFIX/ MOD1: A Computer Program for Fluid-Solids Hydrodynamics, Argonne National Laboratory Report ANL/EES-TM-361, Argonne, Ill., Oct. 1986 (Feb.1989).

Rogers,W.A.(1989). A Model of Erosion in Fluidized Beds Developed Using Kinetic Theory for Granular Flows. DOE Report,DOE/MC/21353-2663.

Stringer,J. and Wright,I.G. (1986). Erosion/Corrosion in FBC Boilers. in *Proceedings of EPRI Workshop on Wastage of In-Bed Surfaces in Fluidized-Bed Combustors*, vol. 1, paper 1.1.

Wood,R.T. and Woodford,D.A.(1983). Effect of Particle Size and Hardness on Material Erosion in Fluidized Beds. in *Proceedings of 6th Int. Conf. in Erosion by Liquid and Solid Impact*, 56.1-56.10.

Zhu,J., Grace,J.R., and Lim,C.J. (1990). Tube Wear in Gas Fluidized Beds— I. Experimental Findings. *Chem. Eng. Sci*, **45**, no.4, 1003-1015.

NOTATION

B_F	defined in eq. (7)
$\mathbf{C}$	fluctuating velocity of particle, m/s
C_d	drag coefficient
$\mathbf{c}$	instantaneous velocity of a particle, m/s
$\mathbf{c}_{12}$	relative velocity of particle 1 and 2, m/s
d_p	particle diameter, m
E	erosion rate, m/s
e	coefficient of restitution
F_1	defined in eq.(13a)
F_2	defined in eq.(13b)
f	particle velocity distribution function
f^2	pair-distribution function
$f(\alpha)$	function defined in eq.(8)
G	solids elastic modulus, Pa
g	acceleration due to gravity, m/s^2
g_0	radial distribution function
$\overline{\overline{\mathbf{I}}}$	unit tensor
K	parameter in Finnie's erosion model, ratio of vertical to horizontal force
$\mathbf{k}$	unit vector along the line from center of particle 1 to 2
m	particle mass, kg
N_{pc}	collision frequency between particles per unit time and unit volume, Hz/m^3
n	particle number density, m^{-3}
$\mathbf{n}$	outer normal direction of a wall
P_H	material hardness, Pa
p	pressure, Pa
$\mathbf{q}$	flux vector of fluctuating energy, kg/s^3
$\mathbf{r}$	space vector, m
$\overline{\overline{\mathbf{S}}}$	deformation rate tensor, s^{-1}
$\frac{3}{2}T$	fluctuating energy, m^2/s^2
t	time,s
U	fluidization velocity, m/s
U_{mf}	minimum fluidization velocity, m/s
$\mathbf{v}$	mean velocity, m/s
v_w	solids phase mean velocity near a wall, m/s
W	volume of target removed by erosion, m^3

Greek letters

α	attack angle, degrees
β	two phase drag coefficient, $kg/s \cdot m^3$
γ	collisional energy dissipation, $kg/s^3 \cdot m$
ϵ,ϵ_s	gas and solids phase volume fraction, $(\epsilon_s = 1 - \epsilon)$
ζ	parameter in Finnie's erosion model, ratio of depth of contact to depth of cut
θ	$= 90^o - \alpha$, degrees

θ_c	$= 90^o - 18.43^o = 71.57^o$
κ	conductivity of granular temperature, $kg/s \cdot m$
ϕ_s	shape factor $(0 < \phi_s \leq 1)$
λ_p	mean distance between particles, m
μ	shear viscosity, $Pa \cdot s$
ξ	bulk viscosity, $Pa \cdot s$
ρ	density, kg/m^3
$\overline{\overline{\tau}}$	stress tensor, Pa
τ	particle-particle collision interval, s

Subscripts

g	gas phase
s	solids phase
w	wall
1,2	particle 1 and 2 or vector component 1 and 2

END

DATE FILMED

9/17/92